Available online at www.sciencedirect.com
SCIENCE DIRECT
Polymer 46 (2005) 9851–9862
polymer
www.elsevier.com/locate/polymer

Introduction of silica into thermo-responsive poly(*N*-isopropyl acrylamide) hydrogels: A novel approach to improve response rates

Kurt Van Durme[a], Bruno Van Mele[a,*], Wouter Loos[b], Filip E. Du Prez[b,**]

[a]*Department of Physical Chemistry and Polymer Science—FYSC (TW), Vrije Universiteit Brussel (VUB), Pleinlaan 2, B-1050 Brussels, Belgium*
[b]*Polymer Chemistry Division, Department of Organic Chemistry, Ghent University (UGent), Krijgslaan 281 S4, B-9000 Ghent, Belgium*

Received 23 December 2004; received in revised form 5 July 2005; accepted 9 August 2005
Available online 21 September 2005

Abstract

The response rates of novel thermo-responsive poly(*N*-isopropyl acrylamide) (PNIPAM) hybrid hydrogels are compared to those of conventional chemically crosslinked PNIPAM hydrogels. The former materials were obtained by applying the sol–gel technology, in which the inorganic silica particles act as physical crosslinks for the organic polymer chains, leading to a semi-interpenetrating polymer network structure. In situ modulated temperature DSC shows that the introduction of hydrophilic silica improves the thermal response rate of the hybrid hydrogels to a great extent as compared to aqueous PNIPAM solutions and conventional PNIPAM hydrogels. Ex situ gravimetrical measurements also illustrate that the shrinking/swelling rate of the hybrid hydrogels is largely improved. It is assumed that the uniform distribution of the SiO_2 units, as demonstrated by cryo-field emission scanning electron microscopy, causes the silica to act as nano-sized water reservoirs, which reduce the characteristic diffusion length of water in the PNIPAM matrix so that it can be transported faster within the hybrid PNIPAM nano-composite.

Keywords: Hydrogels; Poly(*N*-isopropyl acrylamide); Phase separation kinetics

1. Introduction

Thermo-responsive hydrogels have gained much attraction over the last decade because of their large change in properties in response to small temperature variations. Among this family of 'intelligent' thermo-responsive materials, hydrogels based on poly(*N*-isopropyl acrylamide) (PNIPAM), showing a lower critical solution temperature (LCST) at ca. 30 °C, are probably the most studied [1,2]. An important drawback towards the applicability of conventional PNIPAM hydrogels is their response rate, which is usually slowed down due to the formation of a dense skin layer at temperatures above the demixing temperature. This phenomenon retards the outward diffusion of water during the gel collapse process [3]. Therefore the improvement of shrinking/swelling rates has been a major focus of research during the last years. Chu et al. recently published a short overview of several approaches [4].

One possibility to improve the response rate is to prepare a heterogeneous structure of the resulting PNIPAM hydrogel, which reduces the formation of a dense skin layer. This heterogeneous structure can be obtained by several routes: polymerising above the LCST [5–7], using mixed solvents during the polymerisation [8], using a pore forming agent [9,10] or applying a freezing technique, including cold-treatment and freezing synthesis [11,12].

Another approach for preparing fast responsive PNIPAM hydrogels consists of introducing a hydrophilic component, which acts as water channels. Hence the diffusion of water inside the hydrogel is improved. Okano et al. found that introducing freely mobile, grafted poly(ethylene oxide) (PEO) chains on a PNIPAM gel enhanced the shrinking rate [13]. Recently we applied this methodology for poly(*N*-vinyl caprolactam) (PVCL)-based hydrogels, for which both the shrinking and swelling kinetics became instantaneous [14].

Moreover, we combined the thermo-responsive behaviour of hydrogels with the emerging and popular field of

* Corresponding authors. Tel.: +32 2 6293276; fax: +32 2 6293278.
** Tel.: +32 9 2644972; fax: +32 9 2644503.
E-mail addresses: bvmele@vub.ac.be (B. Van Mele), filip.duprez@ugent.be (F.E. Du Prez).

0032-3861/$ - see front matter © 2005 Elsevier Ltd. All rights reserved.
doi:10.1016/j.polymer.2005.08.032

nano-structured materials to design novel hybrid hydrogels. The goal of this work was to apply the sol–gel process for the preparation of nano-structured thermo-responsive hydrogels in order to expand their application area. In general, the sol–gel process consists of hydrolysis, followed by condensation of alkoxy derivatives of metals such as Si or Al, which results in inorganic particles [15].

Starting from an aqueous solution of high molecular weight PNIPAM, reinforced thermo-responsive PNIPAM hydrogels could be prepared by means of this sol–gel concept. As a result the silica particles (nanometer dimensions) act as physical crosslinks for the linear polymer chains. The structure of these materials can be represented as a semi-interpenetrating network (semi-IPN) that consists of a thermo-responsive polymer matrix and a small fraction of silica domains. Despite the fact that there are no covalent crosslinks present in the hydrogels, strong interactions exist between the inorganic silica phase and the organic polymer phase. This is a consequence of both hydrogen bonds and physical entanglements, as schematically depicted in Fig. 1. These new materials can better withstand the mechanical stress produced during the swelling and shrinking processes in comparison with conventional hydrogels. In previous papers the thermo-responsive and improved mechanical properties of these hybrid hydrogels based on PNIPAM [16] or PVCL [17] were discussed.

In the present work the influence of the hydrophilic silica on the response rate of the hybrid hydrogels is investigated by modulated temperature DSC (MTDSC) and ex situ gravimetrical measurements, in comparison with conventional PNIPAM hydrogels. In the study of polymeric materials by means of MTDSC, kinetic thermal processes, depending on time and absolute temperature, often appear in the non-reversing heat flow, while the (specific) heat capacity is found in the reversing heat flow. A complete description of the extraction of the heat capacity and other MTDSC signals can be found in literature [18,19].

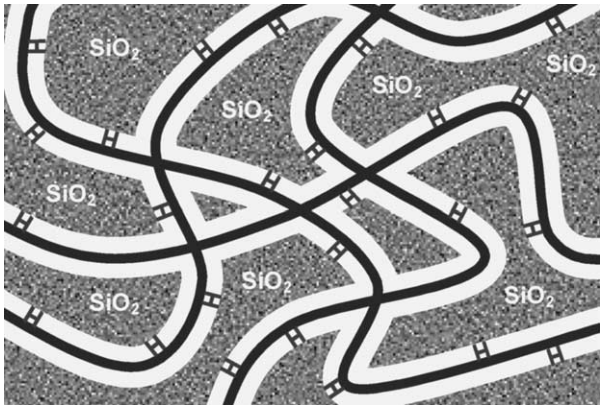

Fig. 1. Schematic presentation of hydrogen bond interactions in PNIPAM hybrid hydrogels. Shaded area, dispersed silica particles; continuous line, PNIPAM chains; H, hydrogen bonds. The PNIPAM chains constitute the matrix, the crossing of the continuous lines represent physical entanglements.

The straightforward deconvolution procedure turns out to be valid for the study of reacting polymer systems [20]. However, it no longer holds for characterizing polymer melting and temperature-induced phase separation in polymer solutions and blends [14,21–25]. Heat effects, coupled with melting/crystallization [21,22] or mixing/demixing [14,23–25], occur during a modulation cycle and thus contribute to the amplitude of the modulated heat flow. Hence, the specific heat capacity in this case is termed 'apparent', c_p^{app}, to distinguish it from the baseline specific heat capacity, c_p^{base}, which is (to a good approximation) only temperature-dependent. The so-called 'excess' contribution, c_p^{excess}, is temperature- and time-dependent and changes with the progress of the transformation:

$$c_p^{app}(T,t) = c_p^{base}(T) + c_p^{excess}(T,t) \quad (1)$$

The ability of MTDSC to study in situ the phase transition behaviour through quasi-isothermal measurements (average heating rate equal to zero) will be utilised in order to obtain information on the kinetics of demixing/(re)mixing and shrinking/(re)swelling of thermo-responsive PNIPAM-based hydrogels. The time-dependencies in c_p^{app} are correlated with ex situ gravimetrical measurements and the observed differences in reponse rate between conventional and hybrid PNIPAM hydrogels are discussed. The morphology of the hybrid hydrogels is analysed by cryo-field emission scanning electron microscopy and transmission electron microscopy.

2. Experimental

2.1. Materials

Tetramethoxysilane (TMOS) (Acros, 99%), 2,2′-azobisisobutyronitrile (AIBN) (Merck-Schuchardt, >98%), ammonium persulphate (APS) (Aldrich, 98%), *N*,*N*,*N*′,*N*′-tetramethylethylenediamine (TEMED) (Aldrich, 99%) and *N*,*N*′-methylene bisacrylamide (MBAA) (Sigma, >98%) were used as received. Benzene (Aldrich, 99+%) was refluxed over a sodium/benzophenone solution. *N*-isopropyl acrylamide (NIPAM) (Acros, 99%) was purified by recrystallisation on hexane, followed by drying under vacuum and storage at 4 °C.

2.2. Synthesis

2.2.1. Linear PNIPAM

The high molecular weight PNIPAM (M_v = 1,580,000 g mol^{-1}) was obtained by radical polymerisation in benzene at 60 °C with AIBN as initiator. The molecular weight was determined by viscosimetry at 25 °C in water, using the Mark–Houwink equation, $[\eta] = KM^a$ with K = 0.0145 mL g^{-1} and a = 0.5 [26]. The glass transition (T_g) of dried PNIPAM is ca. 140 °C.

2.2.2. Chemically crosslinked PNIPAM hydrogels

The conventional PNIPAM hydrogels were prepared by radical polymerisation in distilled water, in which MBAA, APS and TEMED were used as the crosslinker, initiator and accelerator, respectively [27]. In all samples the monomer concentration was 1.525 M, the APS concentration 3.5 mM and the TEMED concentration 15.9 mM. The molar ratio of crosslinker MBAA to NIPAM was either 1/30 (gel1: PNIPAM 1/30), 1/60 (gel2: PNIPAM 1/60) or 1/120 (gel3: PNIPAM 1/120). The mixtures were transferred into glass tubes in which the gelation process was carried out at 10 °C for 24 h. Finally the gels were removed from the tubes and kept in distilled water for 1 week. As such the reaction residues were washed out and equilibrium swelling was achieved. T_g of dried PNIPAM hydrogel is ca. 143 °C.

2.2.3. PNIPAM/SiO_2, physically crosslinked hybrid hydrogels

The synthesis of PNIPAM hybrid hydrogels was carried out in glass tubes containing a magnetic stirring rod. An aqueous PNIPAM solution ($M_v = 1{,}580{,}000$ g mol^{-1}) (pH = 12) is added simultaneously with a certain amount of TMOS. The reaction mixture is stirred for 5 min before being poured between two silylated glass plates, separated by a 1 mm thick spacer. By performing the gelation in a glass mould, the evaporation of water is prevented.

The hybrid hydrogels are described by the initial ratio of PNIPAM/TMOS in wt% in combination with the initial ratio of TMOS to water in the reaction mixture (in wt%). For example: if 0.4 g TMOS is added to a solution of 4 ml water containing 0.4 g PNIPAM (initial TMOS to water ratio is 9.1 wt%), this is noted for convenience as: PNIPAM/SiO_2 50/50 (9.1 wt%) [16]. T_g of dried hybrid PNIPAM hydrogel is ca. 148 °C.

2.3. Preparation of polymer/water solutions and hydrogels

The linear PNIPAM was dried under vacuum for at least 48 h at 130 °C, after which the water content was less than 0.2 wt% as determined by thermo gravimetric analysis (TA Instruments TGA 2950). Starting from a 10/90 (wt/wt%) polymer/water solution, a range of compositions was prepared directly in hermetic Mettler aluminum pans. Samples containing more than 10 wt% polymer were prepared by evaporation of water, while those containing less than 10 wt% polymer by further dilution of the original 10/90 mixture. These samples were stored in the refrigerator for at least 1 week to obtain a homogeneous mixture. A few of the closed crucibles were perforated and the weight loss was measured at 100 °C using TGA to check the preparation procedure (error < 1 wt%).

The network/water samples were prepared directly in hermetic Mettler aluminum pans by adding an excess of distilled water to the swollen network to make sure that the networks were swollen to equilibrium in the homogeneous region; in that case the addition of supplementary water is not leading to further swelling of the networks.

2.4. Modulated temperature differential scanning calorimetry (MTDSC)

MTDSC measurements were performed on a TA Instruments 2920 DSC with the MDSC™ option and on a TA Instruments Q1000 (T-zero™ DSC-technology) with RCS or LNCS cooling accessories. Helium and nitrogen were used as a purge gas (25 mL min^{-1}).

Indium and cyclohexane were used for temperature calibration. The former was also used for enthalpy calibration, while calibration of the heat capacity was performed with water at 20 °C. Data are expressed as specific heat capacities (or changes) in J g^{-1} K^{-1}. For the study of phase separation and phase separation kinetics, not the absolute value, but the changes of the specific heat capacity as a function of temperature and time are important. For this reason, in most MTDSC plots the curves are shifted vertically for clarity. Standard modulation conditions were an amplitude A_T of 0.5 °C with a period p of 60 s. Non-isothermal experiments were performed at an underlying heating rate of 1 °C min^{-1}. Samples of 1–5 mg were introduced in hermetic Mettler aluminum pans. In these conditions the gels swollen to equilibrium had a characteristic size of up to 1 mm.

2.5. Ex situ gravimetrical measurements

The swelling degree of the hydrogels, defined as $S = 100(W_{sw} - W_0)/W_0$ where W_{sw} and W_0 denote the weight of the swollen and dried sample, respectively, was determined gravimetrically. For all ex situ gravimetrical measurements, the networks were first swollen to equilibrium in distilled water in the homogeneous region (e.g. at 20 °C).

To determine the rate of shrinkage, e.g. at 60 °C, the samples were taken out of the water after different immersion times at 60 °C, tapped with filter paper (to remove the excess of water from the sample surface) and weighed (W_{sw}). In this way, the evolution of the swelling degree S was followed by discontinuous ex situ measurements. All samples had a cylindrical size with a thickness of approximately 1 mm.

2.6. Cryo-field emission scanning electron microscopy (cryo-FESEM)

The hydrogel samples were first placed on a Si-wafer and the excess of water was removed with filter paper. Thereafter they were rapidly frozen by plunging into liquid ethane (at ca. −196 °C) to avoid ice crystal formation (i.e. vitreous ice embedding). Freeze–drying was performed during 6 h at approximately −80 °C and 5×10^{-6} Torr using a BAF 300 (Balzers, Liechtenstein) equipped with a turbo molecular pump. Both the freeze- and air-dried

samples were subsequently rotary shadowed at room temperature with 1.5 nm platinum/carbon (Pt/C) at an elevation angle of 65°. Additionally, a unidirectional shadowing with 2.5 nm Pt/C at an elevation angle of 30° was applied to monitor elevated structures. The coated samples were examined with a high-resolution field emission scanning electron microscope ('in-lense' type, S-5000 Hitachi Ltd, Japan) in high vacuum (4×10^{-7} Torr) at room temperature. Micrographs were obtained at 10 kV acceleration voltage, using secondary electrons. The cryo-FESEM micrographs were recorded using Agfapan APX100 photographic film.

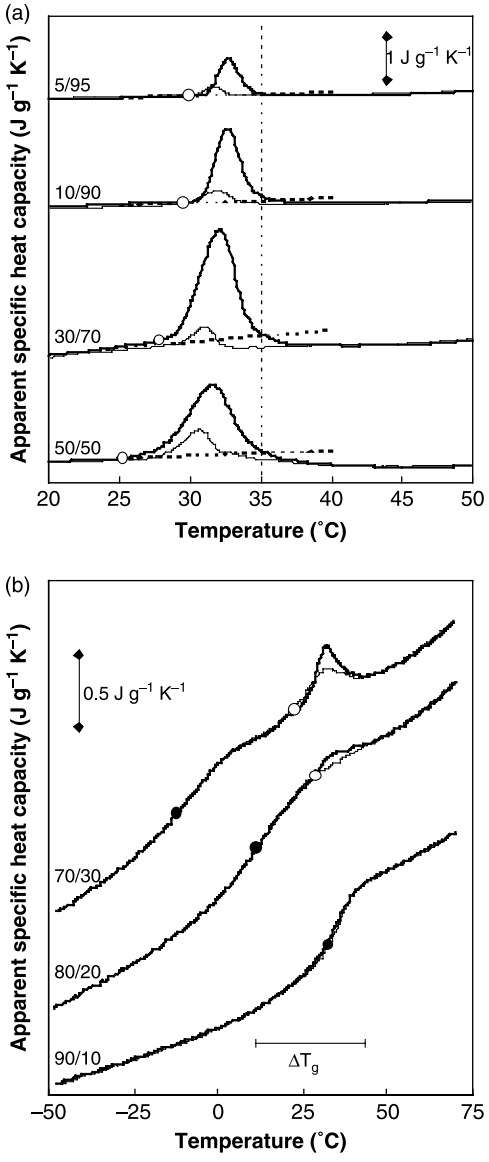

Fig. 2. c_p^{app} during non-isothermal demixing (thick lines) and remixing (thin lines) of PNIPAM 1,580,000/water for different compositions: (a) demixing temperature (○). Dashed line (extrapolated experimental c_p^{base}) is a guide to the eye. Vertical (dashed) line indicates drop of c_p^{app} below c_p^{base} (considered as onset of partial vitrification); (b) demixing temperature (○) and T_g (●). The width of the glass transition (ΔT_g) is indicated for a 90/10 PNIPAM/water mixture. Curves are shifted vertically for clarity.

2.7. Transmission electron microscopy (TEM)

The hydrogels were first dried at room temperature to remove the major part of the water and subsequently they were dried in a vacuum oven at 60 °C. The dry hybrid material was embedded within a low-viscosity resin (LR White Resin, Hard Grade Acrylic Resin, LR London Resin Company Ltd). Ultra thin (50–90 nm) longitudinal sections were cut on an ultramicrotome (Leica, Austria) with a diamond knife (Diatome Ltd, Switzerland) and mounted on form-var coated single slot copper grids (Agar Scientific, UK). A Jeol JEM-1010 (Jeol Ltd, Japan) transmission electron microscope operating at 60 kV was used to take the pictures.

3. Results and discussion

In order to discuss the kinetic properties of the hybrid hydrogels, it is necessary to describe first the mixing/demixing behaviour of aqueous solutions of the pure matrix, i.e. the high molecular weight PNIPAM (1,580,000 g mol^{-1}). The concepts of an MTDSC methodology, thoroughly elaborated in previous work for a low molecular weight PNIPAM (74,000 g mol^{-1}) [24], will be employed to study the effect of the high molecular weight of PNIPAM on the state diagram and especially on the thermal response rate of the building block (matrix) of the hybrid materials. The influence of the inorganic silica phase on the thermo-responsive properties can then be investigated and compared to conventional PNIPAM hydrogels. Both MTDSC (rate of demixing/remixing) and ex situ gravimetrical measurements (rate of shrinking/swelling) are used for this purpose.

3.1. Linear PNIPAM

3.1.1. Non-isothermal demixing and remixing

Upon heating a homogeneous PNIPAM/water solution, phase separation takes place due to a change in molecular interactions [28]. Below the demixing temperature (T_{demix}), intermolecular hydrogen bonding between PNIPAM and water is predominant as demonstrated with attenuated total reflection (ATR)/Fourier transform infrared (FTIR) [29,30] and nuclear magnetic resonance (NMR) [31]. Above T_{demix}, however, hydrophobic interactions between the polymer chains are promoted. This changes the hydration structure around the polymer chains, giving rise to an endothermic heat effect [2,24,26]. By means of MTDSC, the total demixing enthalpy is divided in two endothermic contributions. The largest part, usually more than 90%, is found in the reversing heat flow signal and as such in the heat capacity. Therefore the latter is an 'apparent' specific heat capacity with an 'excess' contribution due to mixing/demixing on the time-scale of the modulation [14,23,24] (Section 1 and Eq. (1)). Consequently, the endothermic

enthalpy contribution in the non-reversing heat flow is usually less than 10% of the total demixing enthalpy.

The evolution with temperature of c_p^{app} is shown in Fig. 2 for different PNIPAM/water mixtures. The start of phase separation upon heating is indicated by the initial deviation of c_p^{app} (thick lines) from the experimental baseline heat capacity, c_p^{base}. By using a threshold value, defined against the extrapolated experimental baseline (Fig. 2(a), dashed lines), the demixing temperature, T_{demix}, of each sample could be obtained (Fig. 2, ○). This approach was previously discussed in more detail for aqueous poly(*N*-vinyl caprolactam) [14], poly(vinyl methylether) [23] and poly(*N*-isopropyl acrylamide) [24] solutions.

Further heating of PNIPAM/water solutions induces partial vitrification of the formed PNIPAM-rich phase, which is seen as a drop in c_p^{app} below the extrapolated experimental c_p^{base} at ca. 35 °C, indicated by a vertical (dashed) line in Fig. 2(a). At much higher temperatures, near the glass transition of the PNIPAM-rich phase, the specific heat capacity again increases towards the extrapolated experimental c_p^{base} (not shown).

Fig. 3 depicts the state diagram of PNIPAM 1,580,000/water determined by MTDSC. T_{demix} (Fig. 2, ○) and the glass transition temperature T_g (Fig. 2(b), ●) are shown for different compositions. The resulting demixing curve has a minimum at off-zero concentration (ca. 50 wt%), which is characteristic for a type II LCST demixing behaviour [2,24,32].

As expected, T_g lowers with increasing water content, due to the plasticizing effect of water on PNIPAM [2,14,24]. The width of the glass transition, ΔT_g, in Fig. 3 is important because the possible interference of partial vitrification during phase separation (indicated by the dotted area) depends on the upper limit of the glass transition rather than

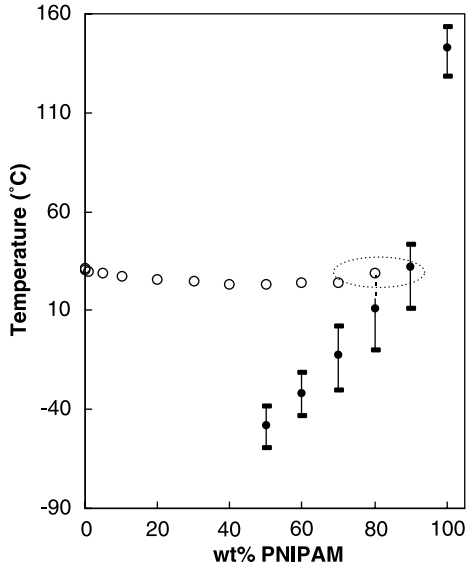

Fig. 3. State diagram of PNIPAM 1,580,000/water: demixing curve (○) and T_g-composition curve (●, width (ΔT_g): I). Demixing temperatures are calculated from threshold in c_p^{app} (0.01 J g^{-1} K^{-1}) upon heating.

on its average value. The calculation of ΔT_g is shown in Fig. 2 for a 90/10 PNIPAM/water mixture.

The remixing kinetics are largely influenced by the thermal history of the preceding phase separation. The temperature and the duration of the demixing step are two important parameters that were thoroughly elaborated in a previous paper [24]. When an aqueous PNIPAM solution is heated above 35 °C, c_p^{app} on cooling (Fig. 2, thin) no longer coincides with the heating curve (Fig. 2, thick). Hence, the reversing remixing exotherm upon cooling is smaller than the reversing demixing endotherm upon heating (in absolute value). This indicates that the rate of remixing is slower than the rate of demixing, due to partial vitrification of the PNIPAM-rich phase. Moreover, the specific heat capacity value after partial remixing (below T_{demix}) is smaller than the initial value of the homogeneous solution. The time needed to completely homogenize the sample at for example 20 °C (i.e. in the homogeneous region) is typically 30 min (after a heating/cooling cycle at 1 °C min^{-1} to 70°C). This is seen as an increase in c_p^{app} towards c_p^{base}, as was also noticed for partially miscible polymer blends with interference of vitrification during demixing [25] and for the PVCL/water system [14]. The longer the mixture is kept at a temperature above the onset of partial vitrification and the higher this temperature (i.e. the higher the degree of partial vitrification of the polymer-rich phase), the slower the remixing process in the homogeneous region: the remixing time at 20 °C can rise up to 1300 min after a demixing at 70 °C for 5000 min [24].

The balance between reversing and non-reversing heat flow contributions is also different upon cooling: the non-reversing heat flow is no longer negligible and mounts up to 60% of the total heat flow. However, the sum of both heat flow contributions upon cooling, i.e. the total remixing enthalpy is in general twice as small as the total demixing enthalpy (in absolute value). This again illustrates that the remixing process was not completed upon cooling.

3.1.2. Quasi-isothermal study: kinetics of partial demixing

The time-dependent behaviour of c_p^{app}, determined by means of quasi-isothermal MTDSC experiments, gives additional information on the phase separation kinetics [14,23–25]. At temperatures below T_{demix}, no time-dependency is noticed, whereas at temperatures above T_{demix}, c_p^{app} becomes time-dependent until a final excess contribution is attained. Fig. 4 depicts a quasi-isothermal demixing measurement at 33.0 °C for several PNIPAM/water compositions. The observed slow decrease in c_p^{app} depends on the polymer concentration. By increasing the amount of PNIPAM from 1 up to 50 wt%, the time needed to achieve an equilibrium varies from a few hours (Fig. 4, 1/99) to a few days (Fig. 4, 50/50, final value not shown). This decrease in c_p^{app} is attributed to morphological changes or an interphase development within the sample. c_p^{excess} is related to enthalpy changes of demixing and remixing on the time-scale of the modulation (fast reversible process). The

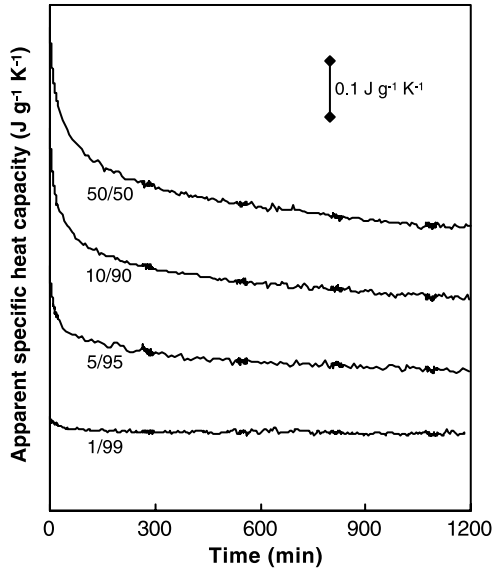

Fig. 4. c_p^{app} during partial quasi-isothermal demixing at 33.0 °C of PNIPAM 1,580,000/water for different compositions, starting from a homogeneous mixture at 15.0 °C heated at 1 °C min^{-1} to 33.0 °C. Time needed to attain an equilibrium: 200 min (1/99), 1050 min (5/95), 3100 min (10/90) and 5000 min (50/50). Curves are shifted vertically for clarity.

polymer/water fraction participating in this fast exchange process slowly diminishes towards an equilibrium. The evolution in $c_p^{excess}(T,t)$ reflects the progress of the phase separation process, associated with a macroscopic morphology development (slow process). The final value of c_p^{excess}, and thus also of c_p^{app} (Eq. (1)), is temperature- and concentration-dependent, but independent of the thermal history of the PNIPAM/water sample [24]. MTDSC thus enables, by means of quasi-isothermal heat capacity measurements, to characterize (i) the fast demixing/remixing reversible processes at the polymer/water interphase of the co-existing phases, and (ii) the slow macroscopic morphology development during phase separation of the aqueous polymer system.

The above-mentioned MTDSC concepts for aqueous solutions will be used to investigate the phase separation and shrinking behaviour of different types of PNIPAM-based hydrogels.

3.2. Chemically crosslinked PNIPAM hydrogels vs. physically crosslinked hybrid hydrogels, PNIPAM/SiO_2

3.2.1. Non-isothermal demixing and remixing

The influence of the SiO_2 particles on the thermal response of hybrid PNIPAM hydrogels will be compared to

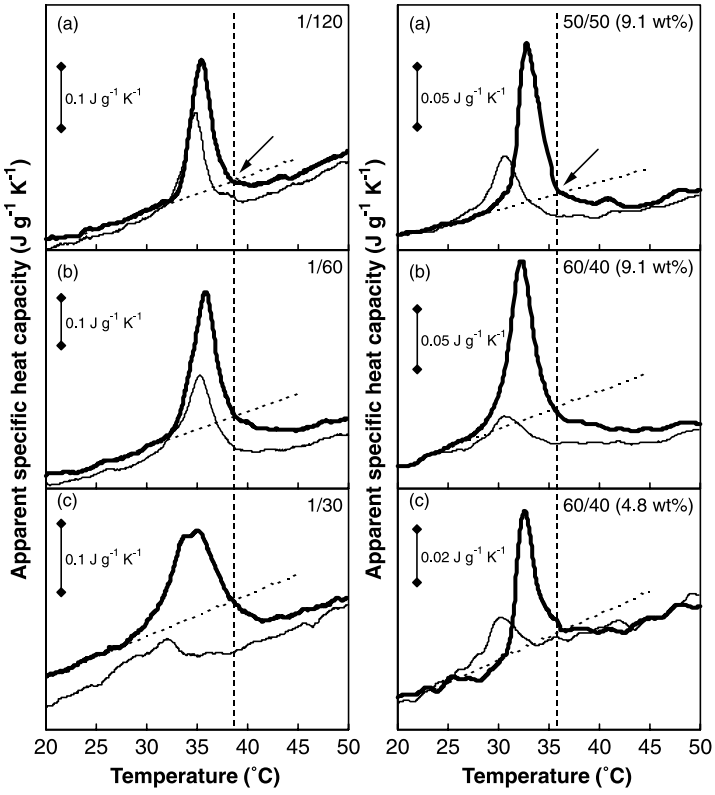

Fig. 5. c_p^{app} during non-isothermal demixing (thick lines) and remixing (thin lines): (left) conventional PNIPAM hydrogels with a crosslink-density of 1/30, 1/60 and 1/120, respectively; (right) hybrid PNIPAM/SiO_2 hydrogels: PNIPAM 60/40 (4.8 wt%), PNIPAM 60/40 (9.1 wt%) and PNIPAM 50/50 (9.1 wt%). Dashed line (extrapolated experimental c_p^{base}) is a guide to the eye. Vertical (dashed) line indicates drop of c_p^{app} below c_p^{base} (considered as onset of partial vitrification). Curves are shifted vertically for clarity.

conventional PNIPAM hydrogels. Fig. 5 (left) shows c_p^{app} during a heating/cooling cycle of three conventional PNIPAM hydrogels, having a different crosslink-density. Initially, all networks were swollen at equilibrium (Section 2).

Upon heating, demixing of the aqueous network (Fig. 5, thick line) is seen as a deviation from c_p^{base}, similar to the linear polymer/water system.

By increasing the crosslink-density, the demixing temperature is lowered from 33.5 °C (PNIPAM 1/120) to 30.5 °C (PNIPAM 1/30), an effect that can be attributed to the initial amount of water present in the swollen network. At 20 °C PNIPAM 1/30 and 1/120 have an equilibrium swelling degree of ca. 650 and 1270%, respectively (Table 1). As a result, the PNIPAM/water ratio is higher in the former hydrogel (ca. 13/87 against 7/93), which leads to a lower T_{demix} according to the state diagram of the linear PNIPAM (Fig. 3), which is representative for that of the network system [2]. In Fig. 5 (left), c_p^{app} drops below the extrapolated c_p^{base} at a constant temperature of ca. 39 °C for all hydrogels (indicated by the vertical dashed line and by the arrow in Fig. 5(a) (left)), again pointing to the start of partial vitrification of the PNIPAM-rich phase in the entire sample.

The typical type II demixing behaviour of the linear PNIPAM is accompanied by a discontinuous shrinking of the PNIPAM hydrogel upon heating [2]. If the diffusion of water out of the hydrogel, in the initial stages of the discontinuous shrinking, is not following the imposed temperature increase, one might anticipate a PNIPAM/water concentration gradient across the hydrogel. Consequently, a dense skin layer can be formed at the outside of the hydrogel as pointed out by several authors [3,7,33,34]. This effect is depending on experimental parameters such as temperature-time combinations (heating rate, step-wise isothermal), initial swelling degree and hydrogel size (characteristic diffusion length) [35,36]. The skin–core effect is thermally induced by phase separation beyond T_{demix} (type II LCST behaviour) and can be interpreted as a spatially localised vitrification of the outer PNIPAM-rich layer. Taking into account the experimental conditions of the non-isothermal MTDSC measurements (underlying heating rate of 1 °C min^{-1}, gels swollen at equilibrium with a thickness of 1 mm or less), the skin–core effect might well be interfering during demixing. In that case, the partial vitrification of the skin layer is probably occurring before the in situ detection of the start of partial vitrification of the entire sample at 39 °C, e.g. around 35 °C as in the case of linear PNIPAM/water (Fig. 2). However, it cannot be detected in c_p^{app} due to the superimposed c_p^{excess} of the ongoing phase separation process at that temperature (Fig. 5 (left)). The vitrified shell is slowing down additional shrinking of the hydrogel upon further heating, because the outward diffusion of water molecules is restricted. As a result, the hydrogel as a whole is no longer at an equilibrium swelling degree and can be considered as a reservoir with a rigid wall, which contains a non-equilibrium amount of water depending on the crosslink-density of the PNIPAM network (see also later). In contrast with the almost arrested shrinking process, the thermally induced demixing still occurs in the inner side of the hydrogel giving rise to a larger fraction of vitrified PNIPAM which is eventually detected in c_p^{app} at 39 °C (see discussion above).

The subsequent (re)mixing upon cooling (Fig. 5 (left), thin line) is also hindered by the vitrified outer layer [34,35], which results in a smaller excess contribution in c_p^{app}. The difference between the heating and cooling curve enlarges as the crosslink-density increases. The difference between the specific heat capacity after partial remixing and the initial value of the hydrogel (swollen at equilibrium below T_{demix}) becomes more pronounced too. On the other hand, all hydrogels showed complete reversibility of the demixing/remixing process, as a second and consecutive heating/cooling cycles (not shown in Fig. 5) coincide with the first cycle of c_p^{app} without an intermediate isothermal period at 20 °C between consecutive cycles. In contrast, for a linear PNIPAM/water system the intermediate isothermal remixing step below T_{demix} is needed for reversibility and coincidence between consecutive cycles [24]. This different thermal response between linear PNIPAM and PNIPAM hydrogel can be explained by the arrested shrinking of the hydrogel during the heating step. Similar effects were noticed by means of conventional DSC [37].

Fig. 5 (right) shows a heating (thick line)/cooling (thin line) cycle of three different PNIPAM/SiO_2 hybrid

Table 1
Equilibrium swelling degree S (%) and amount of water (wt%) at 20 and 60 °C of the conventional PNIPAM and hybrid PNIPAM/SiO_2 hydrogels

Hydrogel	Swelling degree S at 20 °C (wt% H_2O)	Swelling degree S at 60 °C (wt% H_2O)	$\Delta = S_{20\,°C} - S_{60\,°C}$
Conventional PNIPAM			
PNIPAM 1/120	1270 (92.7)	85 (45.9)	1185
PNIPAM 1/60	870 (89.7)	35 (25.9)	835
PNIPAM 1/30	650 (86.7)	35 (25.9)	615
Hybrid PNIPAM/SiO_2			
60/40 (9.1 wt%)	2200 (95.7)	85 (45.9)	2115
60/40 (6.1 wt%)	2700 (96.4)	80 (44.4)	2620
50/50 (9.1 wt%)	2000 (95.2)	270 (73.0)	1730
60/40 (4.8 wt%)	3800 (97.4)	n.a.	n.a.

hydrogels. Demixing in all samples starts at ca. 30 °C, which is again seen as the initial deviation from c_p^{base}. This demixing temperature is somewhat lower than for the previously discussed conventional hydrogels, although the overall PNIPAM/water ratio is smaller (Table 1). A similar decrease in T_{demix} was observed when a PVCL hydrogel was modified with hydrophilic poly(ethylene oxide) grafts [14]. This was explained by the competition between PVCL and PEO to interact with water, which causes a weakening of the PVCL/water interactions in the vicinity of PEO. In this respect, it seems reasonable to assume that the introduction of hydrophilic silica particles also results in a lower value of T_{demix}. Note that the hybrid hydrogels (Fig. 5 (right)) show smaller heat effects than the conventional hydrogels (Fig. 5 (left)). This is caused by the higher equilibrium swelling degrees (2000–3800%) and hence the higher water content (95–97 wt%) of the former gels (Table 1). PNIPAM 60/40 (4.8 wt%), with a swelling degree almost twice as high (3800%) in comparison with both other hybrid hydrogels, shows therefore the smallest heat effect. The effect of partial vitrification upon heating is also less pronounced due to the low content of the hybrid hydrogel in this sample. It should be noted that the start of partial vitrification for all hybrid samples (Fig. 5 (right), vertical dashed line) is detected at approximately the same temperature as for the linear PNIPAM/water systems (ca. 35 °C, Fig. 2(a)). This important observation might indicate that the aforementioned vitrified skin layer is probably not formed in the PNIPAM/SiO_2 hybrid hydrogels (or at least to a much lesser extent), so that the partial vitrification of the polymer-rich phase during demixing might be a one-step process across the entire hydrogel (as it is in the PNIPAM/water system).

The contribution in c_p^{app} upon cooling (Fig. 5 (right), thin line) is again smaller than upon heating (Fig. 5 (right), thick line), which means that the remixing process is still slower than the demixing process. In contrast with the conventional hydrogels, however, the specific heat capacity after partial remixing immediately reaches the initial value of the swollen hydrogel at 20 °C.

The potential of the hydrophilic SiO_2 particles to improve the thermal response rate will be explored in more detail in (quasi-)isothermal conditions using MTDSC and ex situ gravimetrical measurements.

3.2.2. Quasi-isothermal MTDSC study: demixing kinetics

Step-wise quasi-isothermal MTDSC measurements of the chemically crosslinked PNIPAM and the physically

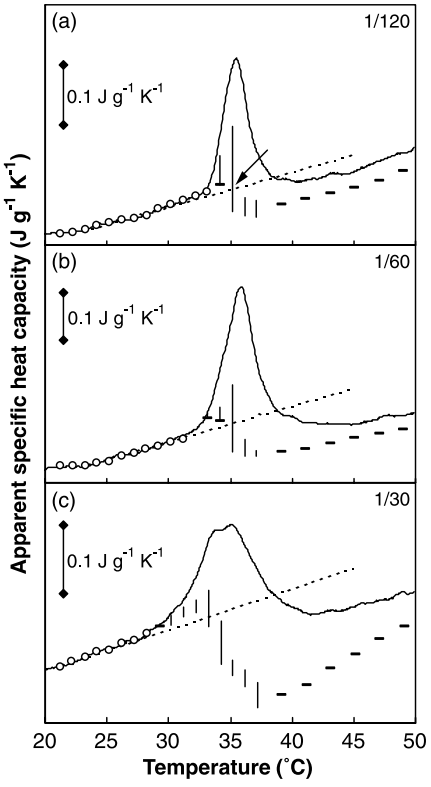

Fig. 6. Overlay of the evolution in c_p^{app} for conventional PNIPAM hydrogels: (a) PNIPAM 1/120, (b) PNIPAM 1/60, and (c) PNIPAM 1/30, heating curve (demixing) and step-wise quasi-isothermal measurements with a step of 1 °C: ○, equilibrium value below T_{demix}; vertical line, time-evolution in c_p^{app} above T_{demix} (—: equilibrium value after 200 min, if no equilibrium is achieved after 200 min: open end). Dashed line (extrapolated experimental c_p^{base}) is a guide to the eye.

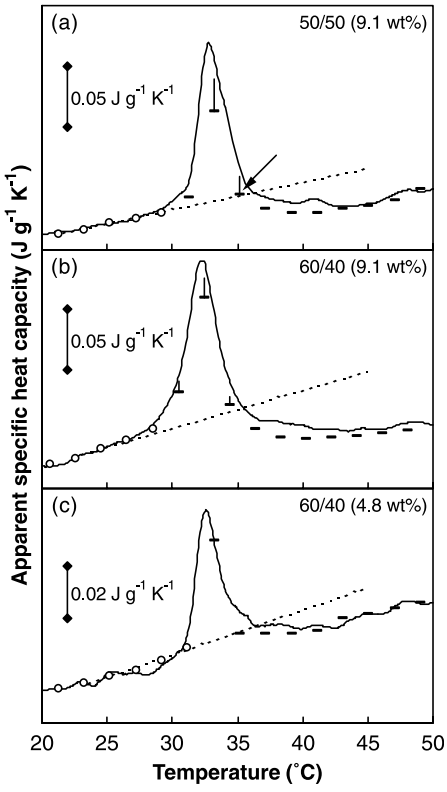

Fig. 7. Overlay of the evolution in c_p^{app} for hybrid PNIPAM/SiO_2 hydrogels: (a) PNIPAM 50/50 (9.1 wt%), (b) PNIPAM 60/40 (9.1 wt%), and (c) PNIPAM 60/40 (4.8 wt%), heating curve (demixing) and step-wise quasi-isothermal measurements with a step of 2 °C: ○, equilibrium value below T_{demix}; vertical line, time-evolution in c_p^{app} above T_{demix} (—: equilibrium value after 200 min). Dashed line (extrapolated experimental c_p^{base}) is a guide to the eye.

crosslinked hybrid PNIPAM/SiO_2 hydrogels are shown in Figs. 6 and 7, respectively. At temperatures below T_{demix}, no time-dependency is noticed. The quasi-isothermal (○) and the non-isothermal values (solid line) coincide, and are corresponding to the baseline specific heat capacities, c_p^{base}, of the hydrogels swollen to equilibrium at the imposed temperature.

At higher temperatures, above T_{demix}, c_p^{app} is not only temperature- but also time-dependent and decreases until a final value is attained, as indicated by vertical lines in Figs. 6 and 7 (if equilibrium is achieved after 200 min: —, if no equilibrium is achieved after 200 min: open end). By connecting the measured final values of c_p^{app} in Fig. 6, it becomes clear that the drop of c_p^{app} below c_p^{base} is detected around 33 °C (arrow Fig. 6(a)), i.e. ca. 6 °C sooner for stepwise quasi-isothermal experiments than in case of heating at 1 °C min^{-1}. This heating rate dependence is also noticed for linear PVCL and PNIPAM aqueous solutions and is caused by the kinetics of phase separation and the influence of the partial vitrification process on it [14,24]. In the case of PNIPAM hydrogels (Fig. 6), the onset of partial vitrification at ca. 33 °C seems a strong confirmation of the suggested localised vitrification in a skin layer during the early stages of phase separation (around 39 °C if heated at 1 °C min^{-1}, see discussion of Fig. 5 (left)).

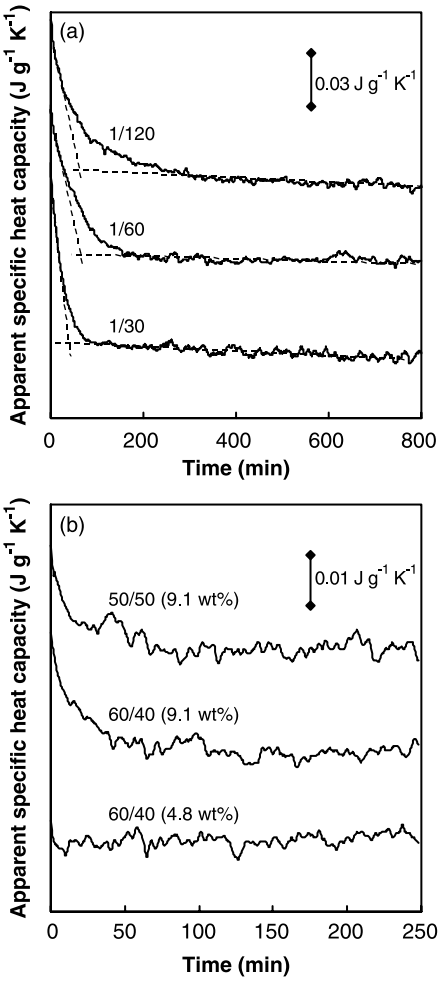

Fig. 8. c_p^{app} during partial quasi-isothermal demixing: (a) at 34.7 °C of conventional PNIPAM hydrogels, starting from a swollen network at 20.0 °C heated at 1 °C min^{-1} to 34.7 °C, dashed lines are a guide to the eye; (b) at 32.7 °C of hybrid PNIPAM/SiO_2 hydrogels, starting from a swollen network at 20.0 °C heated at 1 °C min^{-1} to 32.7 °C. Curves are shifted vertically for clarity.

The effect of the heating rate is less distinct in case of the physically crosslinked PNIPAM/SiO_2 hydrogels (only ca. 1 °C, Fig. 7). Moreover, the observed decreases in c_p^{app} (vertical lines) are also less pronounced and the final values of c_p^{app} below 34 °C still contain an excess contribution, indicating that the hybrid system responds faster than the conventional chemically crosslinked PNIPAM. In the region of partial vitrification above 34 °C, no time-dependency is seen. The PNIPAM 60/40 (4.8 wt%) hydrogel even shows no time-dependency at all over the entire temperature region. The step-wise quasi-isothermal measurements of Fig. 7 are in agreement with a one-step partial vitrification process across the entire hydrogel during demixing (see also discussion of Fig. 5 (right)).

As discussed in Fig. 4, the time-dependency of c_p^{app} beyond T_{demix} is caused by morphological changes or an interphase development in linear PNIPAM aqueous solutions [24], which is also the case for linear PVCL and PVME aqueous solutions [14,23]. Fig. 8 clearly shows that, after heating the hydrogels at 1 °C min^{-1} up to a temperature beyond T_{demix}, the evolution in time of c_p^{app} for (quasi-)isothermal demixing experiments is influenced by the amount and the nature of the crosslinks.

According to the evolution of c_p^{app} in Fig. 8(a), the kinetics of demixing for conventional PNIPAM hydrogels can be characterized by (at least) two stages (indicated by the dashed lines): a fast initial decrease of c_p^{app} is followed by a slow evolution of c_p^{app} for several hours. The difference between the first and the final stage is most pronounced for PNIPAM 1/30 with the highest crosslink-density and the biggest effect of partial vitrification of the entire hydrogel (Fig. 6). A lower crosslink-density results in a smoother transition between both stages. These observations seem consistent with the fact that the hydrogels start to shrink from the surface and the collapsed portion develops from the outer layer towards the inner core [34]. According to this reasoning, the skin layer is probably formed during the heating step at 1 °C min^{-1} up to 34.7 °C. At this temperature, a coarsening process in the still mobile inner part of the hydrogel is going on [3,38], giving rise to a fast decrease of the PNIPAM/water fraction participating in the reversible process of demixing and remixing (fast on the time-scale of the temperature modulation). This morphology development in the core of the hydrogel explains the fast initial decrease of c_p^{excess} and thus of c_p^{app} in Fig. 8(a). The further vitrification of the skin layer towards the core is slowing down the morphology development in the core, leading to the much slower decrease of c_p^{app} in the final stage of Fig. 8(a). This interpretation is tentative and needs

confirmation, e.g. via simultaneous microscopic information on the evolution of the hydrogel structure. However, this is beyond the scope of the present paper, which focuses on the comparison of the thermal response rate of conventional PNIPAM and novel hybrid PNIPAM/SiO_2 hydrogels.

The evolution of c_p^{app} for the hybrid PNIPAM/SiO_2 hydrogels is totally different. Fig. 8(b) shows that both hydrogels containing 9.1 wt% TMOS already reach an equilibrium within the first 2 h. If the hybrid material has a lower crosslink density (4.8 wt% TMOS), no time-evolution in c_p^{app} is seen at all. The kinetics of demixing for the hybrid PNIPAM/SiO_2 hydrogels are characterized by one fast stage without a final slow stage. Note that the rate of demixing of the hybrid hydrogels is much faster than that of the corresponding high molecular weight PNIPAM matrix, i.e. the linear PNIPAM/water 5/95 aqueous solution with a comparable amount of water (Fig. 4). The MTDSC information on the kinetics of demixing will now be compared to that of ex situ gravimetrical measurements on the kinetics of shrinking.

3.2.3. Isothermal ex situ gravimetrical study: shrinking kinetics

The shrinking rate at 60 °C was determined by following the degree of swelling as a function of time via ex situ gravimetrical measurements. The starting materials were hydrogels swollen to equilibrium at 20 °C.

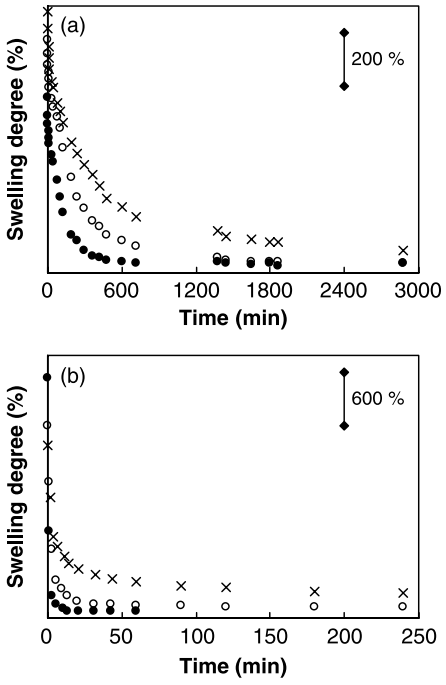

Fig. 9. Change in swelling degree (shrinking) at 60 °C: (a) conventional PNIPAM hydrogels: PNIPAM 1/30, ●; PNIPAM 1/60, ○; PNIPAM 1/120, ×; (b) hybrid PNIPAM/SiO_2 hydrogels: PNIPAM 60/40 (6.1 wt%), ●; PNIPAM 60/40 (9.1 wt%), ○; PNIPAM 50/50 (9.1 wt%), ×.

Fig. 9(a) shows the results for conventional PNIPAM hydrogels and Fig. 9(b) for hybrid PNIPAM/SiO_2 hydrogels, in which analogous trends as in Fig. 8 are noticed. The time needed to attain a final swelling degree after shrinking at 60 °C ranges from ca. 1 day to a few days for the conventional hydrogels (Fig. 9(a)). The change in the rate of deswelling gets smoother with decreasing crosslink-density from PNIPAM 1/30 to PNIPAM 1/120. The previously described interference of the spatially localised vitrification in the skin layer and the subsequent vitrification in the core of the hydrogels is substantially decreasing the shrinking rate.

The hybrid hydrogels shrink much faster at 60 °C (Fig. 9(b)). The gels containing 9.1 wt% TMOS reach an equilibrium within 4–5 h and only a short time-evolution of ca. 10 min is seen for 6.1 wt% TMOS. In contrast with the conventional hydrogels, the influence of partial vitrification of the PNIPAM matrix on the shrinking rate seems negligible for all hybrid hydrogels. Note that there appears to be an optimum ratio between PNIPAM and TMOS, because a higher amount of silica particles (9.1 wt%) results in a slower response rate. In the case of PEO-grafted PNIPAM hydrogels, which also show an improved thermal response rate, an optimum amount of PEO chains was already observed [13].

Another important characteristic of the studied hybrid hydrogels is the fact that the amount of water expelled at 60 °C is at least twice as high as in the conventional hydrogels (Table 1, Δ), while the shrinking rate is much higher. Note that the hybrid PNIPAM/SiO_2 hydrogels also reswell faster than the conventional ones (not shown).

The time scales of the (quasi-)isothermal in situ MTDSC (Fig. 8) and ex situ gravimetrical measurements (Fig. 9) cannot be compared in a straightforward way for several reasons: (i) the different thermal path of the measuring protocol (chosen isothermal temperature and preceding rate of heating); (ii) the dissimilarity in sample size [39], i.e. the gels analysed in MTDSC have typically a 50 times lower weight (although their characteristic thickness, on which the time needed for the diffusion of water depends is similar); (iii) a possible skin–core effect freezing in the shrinking rate at 60 °C in the case of conventional PNIPAM hydrogels (sensed in Fig. 9(a)); (iv) the ability of a progressing morphology development in the core of the conventional PNIPAM hydrogel, even in a situation of an almost arrested shrinking process (sensed in Fig. 8(a)).

Nevertheless, MTDSC and ex situ gravimetrical measurements both clearly indicate that the introduction of silica particles enhances the demixing and shrinking rate of the hybrid PNIPAM/SiO_2 hydrogels. This increased thermal response rate can be explained by a uniform distribution of nano-sized SiO_2 domains in the PNIPAM matrix. The SiO_2-distribution was investigated by means of TEM and cryo-FESEM. The cryo-preparation of the sample in the latter technique is a valuable novel approach for the structural characterization of thermo-responsive hydrogels

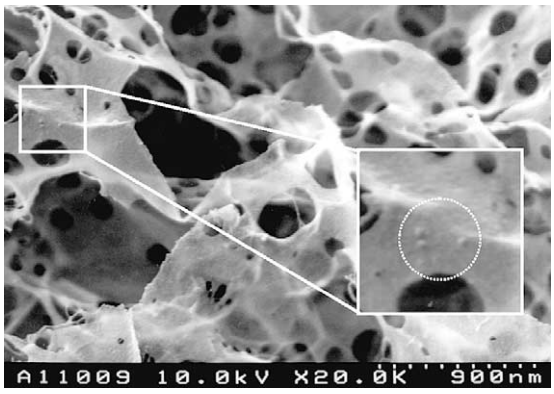

Fig. 10. Cryo-FESEM image of freeze–dried PNIPAM 60/40 (6.1 wt%).

[40]. In this way a reliable image of the thermo-responsive hybrid materials is obtained. Fig. 10 confirms the uniform SiO_2-distribution in the PNIPAM matrix. The silica domains are finely dispersed in the matrix, so that the intrinsic immiscibility of the organic and inorganic phases is on the nanometer-level and no real phase separation is detected (typical for a semi-interpenetrating network), except for some silica particles on the left side of the picture (see inset). Similar images were obtained for all investigated hybrid hydrogels.

Fig. 11 shows a TEM picture of these materials in dry conditions. Although the drying procedure of the gels can induce morphological changes, the uniform distribution of the darker grey spots, representing the silica, confirms the cryo-FESEM results. Note that the uniform distribution of (nano-sized) silica particles is in agreement with the observed T_g rise of approximately 8 °C for the dry hybrid material (i.e. 148 °C against 140 °C for dry PNIPAM), which cannot be anticipated when micro-sized SiO_2 additives are present.

Since the swelling and deswelling rate of a hydrogel is inversely proportional to the square of the distance that the water molecules have to traverse, it is possible to reduce the response time by decreasing the gel dimensions [39]. To reach acceptable response times, it is necessary to decrease the characteristic gel size to the micrometer range or smaller [41]. It is believed that the increased thermal response rate of the hybrid PNIPAM hydrogels is based on this principle.

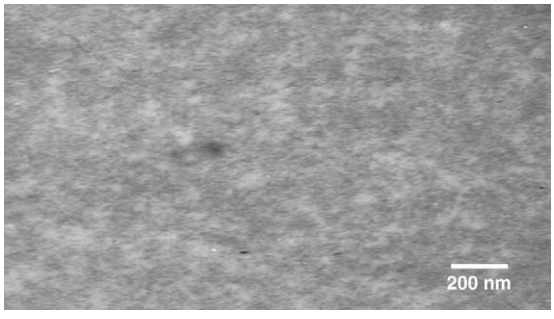

Fig. 11. TEM image of air-dried PNIPAM 60/40 (6.1 wt%).

The structure of these materials can be represented as a semi-interpenetrating network (semi-IPN) that consists of the thermo-responsive PNIPAM matrix and a small fraction of uniformly distributed silica domains acting as nano-sized water reservoirs inside the PNIPAM matrix. The huge interphase region between the inorganic filler and the organic matrix in these nano-composites is dramatically decreasing the characteristic diffusion length of water molecules through the hybrid gels. In this way the nano-sized silica domains have a similar effect on the response rate of PNIPAM hydrogels as hydrophilic PEO grafts [13].

4. Conclusions

Modulated temperature DSC has been used to study the LCST-behaviour and the phase separation kinetics of linear high molecular weight PNIPAM, conventional PNIPAM hydrogels and hybrid PNIPAM/SiO_2 hydrogels. The linear PNIPAM is the matrix polymer for the hybrid hydrogels.

The onset of demixing is determined by the apparent specific heat capacity signal upon heating. The smaller reversing heat flow contribution found upon cooling indicates that remixing is slower than demixing for each studied system.

MTDSC also enables to investigate quasi-isothermally the kinetics of the phase separation process. Depending on the polymer concentration of the linear PNIPAM and on the crosslink density of the conventional PNIPAM hydrogel, the observed time-dependency in c_p^{app} can last several hours (days) before equilibrium is achieved in these slow thermo-responsive systems.

The thermal response rate at any temperature in the phase separation region is increased by the introduction of hydrophilic silica particles, which was demonstrated both in situ with MTDSC (demixing) and ex situ by gravimetrical measurements (shrinking). This can be explained by the higher diffusion rate of water molecules in the interphase surrounding the uniformly distributed SiO_2 domains by a dramatic reduction of the characteristic path length for diffusion.

This novel approach to improve the kinetic properties of thermo-responsive hydrogels by introduction of an inorganic silica phase is promising. By means of the sol–gel concept, a semi-interpenetrating network is formed that consists of a thermo-responsive polymer matrix and a small fraction of silica domains. The silica particles (nanometer dimensions) act both as physical crosslinks for the high molecular weight linear polymer chains and as finely dispersed water reservoirs in the polymer matrix. These nano-composites give rise to fast thermo-responsive hydrogels with a high shrinking capacity in combination with a good mechanical stability [15,16].

Acknowledgements

Prof R. Reichelt from the Institute for Medical Physics and Biophysics at the University of Münster (Germany) is acknowledged for the cryo-FESEM pictures. Prof G. Borgonie and M. Claeys from the Nematology laboratory at Ghent University (Belgium) are kindly thanked for the TEM pictures.

K. Van Durme and W. Loos thank the IWT (Institute for the promotion of Innovation by Science and Technology in Flanders) for a doctoral fellowship. The Stipomat Program of the European Science Foundation (E.S.F.) is acknowledged for financial support.

References

[1] Tanaka T. Polymer 1979;20:1404–12.
[2] Afroze F, Nies E, Berghmans H. J Mol Struct 2000;554:55–68.
[3] Matsuo E, Tanaka T. J Chem Phys 1988;89:1695–703.
[4] Zhang X, Chu C. J Mater Chem 2003;13:2457–64.
[5] Wu X, Hoffmann A, Yager P. J Polym Sci, Part A: Polym Chem 1992; 30:2121–9.
[6] Sayil C, Okay O. Polym Bull 2002;48:499–506.
[7] Takata S, Suzuki K, Norisuye T, Shibayama M. Polymer 2002;43: 3101–7.
[8] Zhang X, Zhang J, Zhuo R, Chu C. Polymer 2002;43:4823–7.
[9] Oxley H, Corkhill P, Fitton J, Tighe B. Biomaterials 1993;14: 1065–72.
[10] Zhuo R, Li W. J Polym Sci, Part A: Polym Chem 2002;41:152–9.
[11] Zhang X, Zhuo R. Macromol Rapid Commun 1999;20:229–31.
[12] Xue W, Hamley I, Huglin M. Polymer 2002;43:5181–6.
[13] Kaneko Y, Nakamura S, Sakai K, Aoyagi T, Kikuchi A, Sakurai Y, et al. Macromolecules 1998;31:6099–105.
[14] Van Durme K, Verbrugghe S, Du Prez F, Van Mele B. Macromolecules 2004;37:1054–61.
[15] Brinker J, Scherer G. Sol–gel science. New York: Academic Press; 1990.
[16] Loos W, Du Prez F. Macromol Symp 2004;210:483–91.
[17] Loos W, Verbrugghe S, Goethals E, Du Prez F, Bakeeva I, Zubov V. Macromol Chem Phys 2003;204:98–103.
[18] Reading M, Luget A, Wilson R. Thermochim Acta 1994;238: 295–307.
[19] Wunderlich B, Jin Y, Boller A. Thermochim Acta 1994;238:277–93.
[20] Swier S, Van Mele B. Macromolecules 2003;36:4424–35.
[21] Minakov AA, Schick C. Thermochim Acta 1999;330:109–19.
[22] Ishikiriyama K, Wunderlich B. Macromolecules 1997;35:1877–86.
[23] Swier S, Van Durme K, Van Mele B. J Polym Sci, Part B: Polym Phys 2003;41:1824–36.
[24] Van Durme K, Van Assche G, Van Mele B. Macromolecules 2004;37: 9596–605.
[25] Swier S, Pieters R, Van Mele B. Polymer 2002;43:3611–20.
[26] Boutris C, Chatzi EG, Kiparissides C. Polymer 1997;38:2567–70.
[27] Hoffman AS. Adv Drug Deliv Rev 2002;43:3–12.
[28] Schild HG. Prog Polym Sci 1992;17:163–249.
[29] Lin SY, Chen KS, Run-Chu L. Polymer 1999;40:2619–24.
[30] Ramon O, Kesselman E, Berkovici R, Cohen Y, Paz Y. J Polym Sci, Part B: Polym Phys 2001;39:1665–77.
[31] Ohta H, Ando I, Fujishige S, Kubota K. J Polym Sci, Part B: Polym Phys 1991;29:963–8.
[32] Šolc K, Dušek K, Koningsveld R, Berghmans H. Collect Czech Chem Commun 1995;60:1661–88.
[33] Suzuki A, Yoshikawa S, Bai G. J Chem Phys 1999;111:360–7.
[34] Zhang X, Zhuo R, Yang Y. Biomaterials 2002;23:1313–8.
[35] Shibayama M, Nagai K. Macromolecules 1999;32:7461–8.
[36] Suetoh Y, Shibayama M. Polymer 2000;41:505–10.
[37] Shibayama M, Suetoh Y, Nomura S. Macromolecules 1996;29: 6966–8.
[38] Shibayama M, Morimoto M, Nomura S. Macromolecules 1994;27: 5060–6.
[39] Kuckling D, Adler HJ, Arndt KF, Hoffmann J, Plötner M, Wolff T. Polym Adv Technol 1999;10:345–52.
[40] Arndt KF, Schmidt T, Reichelt R. Polymer 2001;42:6785–91.
[41] Kuckling D, Harmon ME, Frank CW. Macromolecules 2002;35: 6377–83.